Journal of Computer Science

Research Article

Enhanced Lifetime Maximization Using Metaheuristics-Based Unequal Clustering With Routing Protocol on Wireless Sensor Networks

N. E. Kanaghadhara and R. Suban

Department of Information Technology, FEAT, Annamalai University, Chidambaram, Tamil Nadu, India

Article history
Received: 02-05-2026
Revised: 25-05-2026
Accepted: 15-06-2026

Corresponding Author:
N. E. Kanaghadhara
Department of Information Technology, FEAT, Annamalai University, Chidambaram, Tamil Nadu, India
Email: kanaghadharaphd@gmail.com

Abstract: The Wireless Sensor Network (WSN) consists of spatially distributed autonomous sensors that monitor environmental or physical factors such as sound, pressure, or temperature, and pass the information directly through the network to a sink or central location. Clustering and routing are essential in WSNs to optimize their longevity, scalability, and efficiency. Clustering includes grouping Sensor Nodes (SN) into clusters, each containing a designated Cluster Head (CH) that transmits and aggregates data to the sink. This decreases the transmission overhead and conserves energy, as only the CHs interact over longer distances. On the other hand, routing is a procedure of defining the optimum path for the data transmission from SNs to the sink. Dynamic routing ensures timely and reliable data transmission while balancing the network load and reducing energy consumption. Metaheuristic algorithms play an important role in enhancing clustering and routing. WSNs can obtain better clustering and routing by leveraging metaheuristics, which results in extended operational lifetimes and improved network performance. Thus, the study presents a metaheuristic-based unequal clustering with routing protocol for lifetime maximization (MBCRP-LFTM) technique in WSN. The presented MBCRP-LFTM technique enhances the energy efficiency and lifespan of WSNs utilizing cluster-driven routing approaches. In the MBCRP-LFTM technique, an Iteration-assisted Enhanced Mother Optimization Algorithm (IEMOA) based clustering model offers an effective CH selection and unequal cluster construction. Besides, the IEMOA-based unequal clustering technique designs an objective function comprising multiple input metrics such as residual power level, CH balancing factor, and inter- and intra-cluster distance. Meanwhile, the MBCRP-LFTM technique designs a lotus effect optimization algorithm (LEA) based routing model to pick optimal routes to the sink. The LEA technique selects optimal routes using a fitness function comprising energy efficiency and link quality. An extensive series of simulations was conducted to show the efficiency of the MBCRP-LFTM method. The experimental outcomes reported that the MBCRP-LFTM model achieves improved performance compared to more recent techniques.

Keywords: Wireless Sensor Network, Metaheuristics, Unequal Clustering, Routing, Lotus Effect Optimization, Sensor Node

Introduction

A Wireless Sensor Network (WSN) consists of low-cost, low-power, and versatile wireless sensors able to execute wireless communication, computing, and sensing (Darabkh et al., 2019). These sensors are deployed at random. These nodes need to configure themselves into a wireless network and achieve a particular activity once they are deployed (Fang et al., 2021). Because sensors have limited power, the battery is the main source of WSN. LEACH is a cluster-based algorithm in which every node is occasionally chosen to be a (CH). Sensors are interconnected to transmit important information regarding the actual environment (Sharma et al., 2017). Every node collects data and communicates to the Base Station (BS). Sensors do not want to transmit data concurrently; they may forward it individually through neighboring nodes. WSN is efficient, simple, and reliable to use. Sensors in WSNs constantly utilize batteries (Tandon et al., 2021). Due to the network of devices, recharging the batteries is difficult, and the batteries' capability appears as the most valuable resource for WSN. As a result, energy maintenance causes an important problem in WSN. A novel optimization process needs to be developed to increase energy efficiency and network lifetime (Arjunan and Pothula, 2019). Clustering is the power management function of WSN that divides the network into various clusters, with a single node in every cluster selected as the CH. The CH can decrease the complexity of the BS through the data aggregation process. Since the BS receives data from the least number of nodes, the WSN conserves power in the resource-limited environment. Therefore, the clustering process helps to decrease power utilization in the system.

The distribution of CHs becomes non-uniform because it doesn't react to variations in node density or traffic patterns, leading to quick energy depletion between particular nodes when the remaining nodes stay inactive. The unequal clustering technique offers adaptive node distribution and traffic load balance in response to this problem (Arjunan and Pothula, 2019; Arjunan and Sujatha, 2019). The routing procedure plays the most important role in the lifespan of the sensor nodes (Ramachandran and Perumal, 2018). Routing in WSN cannot be comparable to other wireless networks due to numerous special features of sensor nodes such as processing capabilities, energy restrictions, transmitting gathered data from various nodes to a single base station, uncertainty of global addressing, casual distribution of sensor nodes, etc. To address these types of characteristics, various forms of routing procedures were prepared (Daniel et al., 2021). Mainly two sets of protocols, flat and hierarchical, are used. Each node plays an equivalent role in flat routing protocols. The major problems in flat routing protocols are route support, load balancing, scalability, and not being possible for larger networks (Wang et al., 2018). To handle both load balancing and scalability problems in flat routing, hierarchical routing protocols are presented. Each sensor node in the network is divided into layers based on residual energy and allocated to different parts, otherwise called cluster-based routing (Tam et al., 2018). Various forms of clustering and routing protocols with different issues are deployed to develop energy-effective WSNs.

The major contributions of the MBCRP-LFTM technique are that it employs an iteration-assisted Enhanced Mother Optimization Algorithm (IEMOA) based clustering technique for effective CH selection and unequal cluster construction. Besides, the IEMOA-based unequal clustering technique designs an objective function comprising multiple input metrics such as residual energy, CH balancing factor, and inter- and intra-cluster distance. Meanwhile, the MBCRP-LFTM technique designs a lotus effect optimization algorithm (LEA) based routing model to pick optimum routes to the sink. The LEA technique selects optimal routes using a fitness function comprising energy efficiency and link quality. A comprehensive set of simulations was conducted to display the efficiency of the MBCRP-LFTM system.

Literature Survey

Roberts et al. (2018) suggest an enhanced two-phased method for cluster-based routing, energy-efficient, in the WSN model. The proposed system incorporates two developed Meta-Heuristic (MH's) algorithms: Spotted Hyena Optimization (SHO) and Sailfish Optimization (SFO). This united method influences SFO's quick investigation for effective clustering and optimum CH selection. In addition, SHO's refined utilization abilities improve effective routing paths. In Kumar et al. (2023), an effective Type-II Fuzzy Logic through Butterfly Optimizer-Based Route Selection (TFL-BOARS) is proposed for clustered WSN. The TFL-BOARS method includes the T2FL method with different input limits to pick CH and build clusters. Again, the BOARS method is used to pick the optimum group of routes. Subramani et al. (2022) concentrate on planning the MH-based clustering with a routing algorithm for underwater WSN (UWSN), called MCR-UWSN. However, the multihop routing method, parallel to the grasshopper optimizer (MHR-GOA) method, is received through several input parameters.

Sahoo and Sabyasachi (2022) introduce the cluster-based BAT system for energy harvesting (CBA-EH) method in IoT-enabled WSNs to increase network execution. BAT is used to enhance the strength factors related to CH selection. The usage of EH-allowed nodes allowed us to efficiently control and reduce the system's operating expenses. Chaurasia and Kumar (2023) designed a Metaheuristic-based Optimized Opportunistic Routing Protocol used for WSN (MOORP) based on a better optimum forwarder node selection method and dragon-fly routing optimization technology. The forwarder node selection has been enhanced to consider residual power and Euclidean distance of the nodes. The route from the forwarder to the target is identified using the Dragon-fly algorithm. MOORP applies a Route Searching Algorithm (RSA) along with an Energy Level Matrix upgrade utilized to enhance the routing conclusion. Mohan et al. (2022) proposed an enhanced metaheuristic-based gathering over a multi-hop routing procedure for a submerged WSN, termed the IMCMR-UWSN method.

He et al. (2024) implemented an energy-efficient clustered and multi-hop routing procedure with the metaheuristic-based method to increase the energy efficiency in UWSN and lengthen the network's life cycle. Nevertheless, the current metaheuristic-based technology utilizes two different algorithms to cluster and multi-hop routing with dissimilar initialization, increased computing difficulty, and trouble in hyperparameter tuning. This article proposes a unique hierarchical framework named Hierarchical Chimp Optimizer (HChOA) for both cluster and multi-hop routing procedures. Barnwal et al. (2023) concentrate on designing a Metaheuristics Cluster-based Routing Method for an energy-efficient WSN (MHCRT-EEWSN) Model. The following methods apply the Whale Moth Flame Optimization method, which could be applied with the usage of a fitness function connecting energy, balanced factors, and inter- and intra-cluster distance. In addition, the MHCRT-EEWSN models incorporate an Improved African Buffalo Optimizer (IABO) based routing method. For choosing an optimal route in WSN, the IABO algorithm plans well-being functions including several limits.

While some clustering and routing protocols have been developed for Wireless Sensor Networks (WSNs), the existing approaches are still plagued with significant issues, including energy imbalance, sub-optimal load balancing, higher routing overhead, and scalability problems in large-scale deployment scenarios. Most clustering methods are unable to achieve optimal clustering stability because they use inefficient CH selection methods, and routing protocols involve more energy-consuming non-adaptive route optimization strategies. Additionally, some recent "metaheuristic-based" methods optimize the cluster formation or routing independently, but not a framework that can work together to optimize both the cluster formation and routing for a long network lifetime. There are also methods available that consider the tradeoff of the intra-cluster communication cost, residual energy preservation, and routing link quality to a limited extent. Thus, an efficient hybrid optimization-based unequal clustering and routing system that can enhance the energy efficiency, network stability, and maximize the network lifetime in a WSN environment is required.

Methods

In the research, we have proposed a novel MBCRP-LFTM technique in WSN. The presented MBCRP-LFTM technique improves the energy efficiency and lifespan of WSNs using unequal cluster-based routing approaches. The motivation for using the IEMOA and LEA algorithms in the proposed framework is due to their speed of convergence, strong optimization ability, and exploration–exploitation balance. The IEMOA algorithm is very well suited for unequal clustering due to its effectiveness in achieving optimal cluster head positions and balancing cluster formation and minimum communication overhead. Moreover, the adaptive iterative search mechanism of IEMOA ensures the stability of convergence and avoids local optima trapping.

In the meantime, the LEA algorithm is used for the routing optimization as it has an efficient capacity for neighbourhood exploration and adaptive route selection. LEA is able to accurately find energy-efficient and high-quality communication paths through the consideration of residual energy and link quality, as well as routing fitness metrics. Fig. 1 demonstrates the entire flow of the MBCRP-LFTM technique.

System Model

WSN continuously monitors the physical condition of the surroundings (Cherappa et al., 2023). The architecture of WSN includes several SNs and a BS.

Network Model

The main objective of WSN clustering is to decrease the power utilization by separating the sensors into clusters. The nodes rapidly monitor their surroundings and transfer information to the CHs. The CH nodes are often selected among these nodes. The important role of the CH is to collect information from every node of the cluster and transmit it to the BS. The clustering procedure helps in avoiding direct connections among sensors and receivers.

Energy Model

Once the threshold distance (n) surpasses the n' values, the node power is directly proportional to the broadcast distance n' . The formulation shows the complete energy used by all the nodes to transfer the $'M'$-bit data packets:

$$E_{tx}(M,n) = E_{elec} \times M + \varepsilon_{am} \times M \tag{1}$$

$$\varepsilon_{am} = \begin{cases} \varepsilon_f \times n^2, when\ n \leq n_0 \\ \varepsilon_p \times n, when\ n > n_0 \end{cases} \tag{2}$$

Where as E_{tx} represents the complete power utilized for the communication of data, *Elec* signifies the energy loss per bit, ε_f indicates the power consumed to increase in the open space model, M indicates the number of bits, and n_0 represents the threshold broadcast distance.

The energy depletion of receivers is denoted as follows:

$$E_{rx}(M) = E_{elec} \times M \tag{3}$$

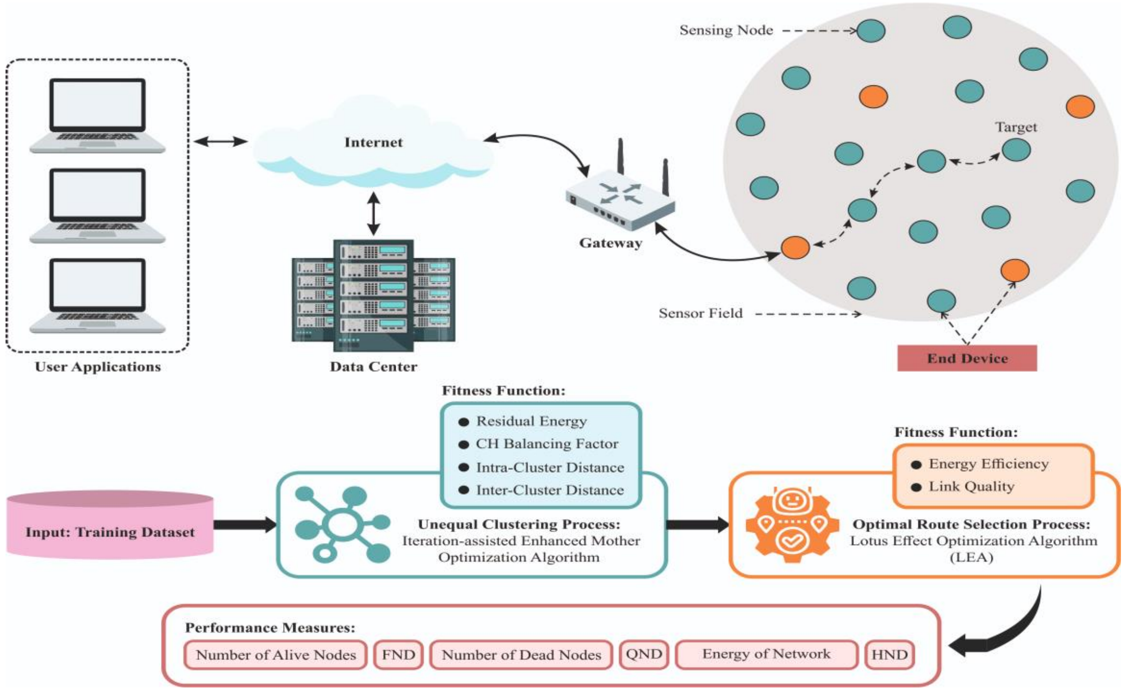

Fig. 1: Overall flow of the MBCRP-LFTM technique

$$E_{sum} = E_{rx} + E_{tx} \tag{4}$$

In Eqs. (3) and (4), E_{rx} refers to the overall energy needed for receiving the information, and E_{sum} is the overall energy loss for the WSNs.

K-Medoids With CH Selection

The SN is ordered into clusters employing the cluster method, and a CH is nominated for every cluster in the WSN. The fundamental task of a CH is to collect data from certain cluster nodes and transmit it to the BS. The Above study presents a K-medoids technique for WSN clustering. The K-medoids divide each SN into k clusters. All the clusters are related to a single object. The object identified is known as a medoid and corresponds to the central point of the cluster. The K-medoid cluster is the shortest distance among clusters since the K-medoid associated with the cluster nodes discovers the optimal center. It increases connection among SNs, decreases energy usage, and identifies precise cluster centers, which leads to short packet delay. The K-medoids approach is effective and has a defined number of steps. The clustering algorithm of K-medoids contains the following steps:

Step 1: Choose k points arbitrarily from the input dataset (k indicates the number of clusters).

Step 2: The data point is allocated to the cluster that has the nearest center point.

Step 3: For each data point in the i^{th} cluster, evaluate the distance to each data point. Identify the point of the i^{th} cluster that decreases the overall distance evaluated from each point as the cluster center point.

Step 4: Repeat steps 1 and 3 till convergence is met.

The clustering approach includes grouping SNs and selecting CHs for every group in the WSNs. The main task of a CH is to gather data from certain cluster nodes and transfer it to the BS. Cluster formation can be achieved using K-medoids due to its capability in finding accurate central clusters, or centroids, which leads to low packet latency, better SNs, and less energy consumption. The process involves calculating the 1st CH node and estimating the number of clusters based on Eq. (5):

$$c = \sqrt{\frac{n}{2}} \tag{5}$$

In Eq. (5), n shows the node count. This algorithm determines the first mean value point and center location (L) for each node:

$$L = \frac{\Sigma_{n=1}^{N} x_n}{n} \tag{6}$$

In Eq. (6), x_n is the sensor coordinate. The average distance between SN and L is shown as D:

$$D = \frac{\Sigma_{n=1}^{N} |x_n - L|}{n} \tag{7}$$

The segregation between SN and the center location

(L) is used for calculating the centroid, and clustering can be attained by Eq. (7) until an appropriate CH is chosen.

Algorithmic Design of IEMOA

Primarily, the MBCRP-LFTM technique takes place; the IEMOA-based unequal clustering technique is presented for effective CH selection and cluster construction. The study alters a present MOA to attain amazing precision and faster convergence when compared to other meta-heuristic models (Abidi et al., 2024). The mathematical equation is presented in Ep. (8):

$$\lambda = -t * \frac{1}{\text{Max}_{iter}} \tag{8}$$

Where the randomly generated variable is specified as λ . Max_{iter} describes the maximum iteration, and τ represents the present repetition. The arbitrary variable is updated in the suggested IEMOA. The numerical method of the recommended IEMOA is defined as follows.

The home is the former education organization, and the mother plays the role of teacher, which is vital while developing kids. A mother used to tell valuable life lessons to her kids, and they grow up as a result of her guidance. The 3 most major methods that a mother and her kids are involved in are guidance, training, and nurturing. Therefore, the recommended MOA creates the benefit of computational modeling of sympathetic and useful activities. The proposed MOA is a population-level meta-heuristic model, which utilizes an iterative model to challenge optimization problems. The origin of the technique is based on latent fixes, which are exposed as variables in the space of the problem. Eq. (9) signifies the matrix method of the population. Initialize the optimizer process utilizing Eq. (10):

$$U_i = \begin{bmatrix} U_1 \\ \vdots \\ U_i \\ \vdots \\ U_s \end{bmatrix}_{s\times m} = \begin{bmatrix} U_{1,1} & \dots & U_{1,d} & \dots & U_{1,m} \\ \cdots & \ddots & \vdots & \vdots & \vdots \\ U1 & \dots & U_{i,d} & \dots & U_{i,m} \\ \vdots & \vdots & \vdots & \ddots & \vdots \\ U_{s,1} & \dots & U_{s,d} & \dots & U_{s,m} \end{bmatrix}_{s\times m} \tag{9}$$

$$u_i, = \gamma_j + \lambda.\left(\gamma_j - \kappa_i\right), i = 1,2 \dots\dots s, j = 1,2 \dots\dots m. \tag{10}$$

Where as s denotes the number of participants in the population, m signifies the sum of vital factors, and U refers to the matrix amount of population. The variable λ delivers the random range which lies among $(0,1)$. Similarly, the lower and upper bounds are represented as γ_j and κi . The U_i is equivalent to $U_i = u_{1,i} \dots . u_{1,j} \dots . . u_{i,m}$.

Every member in the MOA population provides a probable solution to the issue below the optimizer, and the value that every module of the cluster recommends for the decision variable is employed in order to compute the objective value. The function parameter is stated as a vector by using Eq. (11):

$$K = \begin{bmatrix} K_1 \\ \vdots \\ K_i \\ \vdots \\ K_s \end{bmatrix}_{s\times 1} = \begin{bmatrix} K(y_l) \\ \vdots \\ K(y_i) \\ \vdots \\ K(y_S) \end{bmatrix}_{s\times 1} \tag{11}$$

Here, K refers to the objective function value for $the\ ith$ candidate, and K_i denotes a group of non-biased parameter values.

Stage 1: Training (examination stage): Using Eq. (5), an additional location is made for each distinct value throughout this stage. As Eq. (6) establishes, the novel position is known as a proper associate's location if the objective function increases:

$$U_{i,j}^{p_1} = \left(u_{i,j}^{p_1} + \lambda_{(0,1)}\right).\left(l_j - \lambda(2).u_{i,j}^{p_1}\right) \tag{12}$$

$$U_i = \begin{cases} \{u_i^P, T_i^P < K_i \\ u_i^P, else \end{cases} \tag{13}$$

Where as $K_{i,j}$ denotes the j_{th} part of the initial point of $the\ i_{th}$ demographic applicant, and T_i represents the mother location. The $K_{i,j}$ is obtained for the i_{th} population member utilizing primary MOA. The $\lambda(2)$ describes the arbitrary function, which evenly produces a randomly generated integer from $(1\ and\ 2)$. Here, λ denotes the randomly generated integer; in traditional methods, the random even integer is formed utilizing the interval of $(0\ and\ 1)$. This leads to optimization problems, and the utilization of the projected formula in Eq. (8).

Stage 2: Guidance (exploration stage): Every individual group of poor behavior, $KKl_{i,j}$, is discovered by using Eq. (14) in order to equate the objective function value. A module is evenly selected randomly from the generated group of annoying actions, $KKl_{i,j}$, for every $u_{i,j}$. Utilizing Eq. (15), a novel position is first constructed for every member to prevent the kid from damaging actions. The additional location arises from the linked individual's preceding part, as defined by Eq. (16):

$$JJ_i = \{u_k, K_\gamma > K_i \in l\{1,2, \dots . s\}, whereas\ i = 1,2 \dots . s \tag{14}$$

$$u_{i,j} = u_{i,j} + \lambda.\left(u_{i,j} - \lambda(2).KKl_{i,j}\right) \tag{15}$$

$$U_i = \begin{cases} \{u_i^P, K_i^P < K_i \\ u_i^P, else \end{cases} \tag{16}$$

In the above-mentioned equations, the term $KKl_{i,j}$ is the selected unwelcome behaviour for the i_{th} population member; $KKl_{i,j}$ is its j_{th} size, and $u_{i,j}$ denotes the group of worst behaviour for the i_{th} group associate.

Stage 3: Nurturing (manipulation stage): Generally, mothers use to cheer their kids to improve their potential during their education in an assortment of methods. With a little change in the population member location, parenting improves area exploration and exploitation ability throughout the MOA stage. Every group member is assumed to be in a novel location depending upon the formation of children's behavior evolution with the aid of Eq. (17). If the objective function value improves in the novel location, the currently formed location is replaced with the previous one, followed by the corresponding follower, as stated in Eq. (18):

$$u_i^{p1} = u_i^{p1} + \gamma \times (1 - 2\lambda) \frac{\times(\gamma_j - \kappa_i)}{m} \quad (17)$$

$$u_i = \begin{cases} \{U_i^P, K_i^P < y_i \\ U_i^P, else \end{cases} \quad (18)$$

Here, U_i^P denotes the novel position defined by the 3rd phase; the term U_i^P represents the i_{th} member of the population. While i refers to the outcome of the objective function, m signifies the accurate worth of the repetition counter.

Design of IEMOA-Based Unequal Clustering Approach

Besides, the IEMOA-based unequal clustering technique designs an objective function comprising multiple input metrics such as residual energy, CH balancing factor, and intra-cluster and intra-cluster distance. The parameter is in charge of the derivation of the Fitness Function (FF). The FF can be evaluated for the CH selection (Vaiyapuri et al., 2022). This ensures that the node positioned near the BS has more possibilities for CH selection and the node has the maximum energy.

Average Intracluster Distance (f1)

The intra-cluster space is the sum of the spaces among the SNs and CHs. It must be reduced to decrease the power utilization. It is supplied since SNs consume energy when communicating with the CH:

$$f_1 = \sum_{j=1}^{m} \left(\frac{1}{lj} \sum_{k=1}^{lj} dis\left(s_{k,CH_j}\right)\right) \quad (19)$$

Average Sink Distance (f2)

The distance between the BSs and the CH for all SNs in the corresponding CH is used to calculate the average distance of the sink node. Space has a great influence on energy usage; later, these parameters are considered. Thus, it is essential to reduce the distance for power saving:

$$f2 = \sum_{j=1}^{m} (\frac{1}{lj} dis(CH_j, BS)) \quad (20)$$

Residual Energy (f3)

There is a necessity to decrease energy usage since a network's lifecycle is based on energy consumption. Consequently, this parameter is measured. It is assessed as the number of the given channels' existing power. All the objective functions are balanced by the opposite because the total power must be decreased:

$$f3 = \frac{1}{\sum_{j=1}^{m}(E_{CHj})} \quad (21)$$

CH Balancing Factor (f4)

The cluster should be stable; there is a possibility that a few small and large groups form the random grouping of SNs. Thus, these characteristics are reflected while balancing energy usage:

$$f4 = \sum_{j=1}^{m} \frac{n}{m} - l_j \quad (21)$$

The FF is given as follows:

$$Fitness\,function = (p \times f1) + (q \times f2) + (f3 \times r) + \big(f_4 \times (1 - p + q + r)\big), \quad (23)$$

In Eq. (23), q and r are the constant values, and $p + q + r$ 1. The weighting parameters *(p, q, r)* were used to achieve a tradeoff between the different clustering goals, including minimization of communication distance, efficiency of clustering, and residual energy preservation. The proper choice of these weighting coefficients helps to avoid premature energy consumption of cluster heads and equal energy usage among cluster heads in the network. The adopted weighting approach achieves the stability of clusters and maximizes network lifetime, which is achieved by jointly considering the communication efficiency and node energy conditions.

Overview of LEA

Meanwhile, the MBCRP-LFTM technique designs an LEA-driven routing method to take optimum routes to the sink. The lotus effect is described as self-cleaning and super-hydrophobic features of leaves (Rao and Sundar, 2024). This LEA algorithm has two stages: Extraction and exploration. During exploration, the insect's activities, such as dragonfly (DF) and seed-spreading actions, are applied. During extraction, the flower buds grouped near a center point could motivate a neighbourhood-based search strategy, which uses multiple populations and search properties. The DF causes leaf pollination. The DF algorithm is simulated by the LEA strategy. In this phase, the food and enemy behaviors of the DF are efficiently used to define the optimum solution. The DF location is updated by the escaping strategy from food-searching activities and enemies. Using Eq. (24), the location of an individual can be measured:

$$T_j^u = -\sum_{k=1}^{o}(Y_j^u - Y_k^u) \tag{24}$$

Where Y_j indicates the existing location. The k shows the index. u represents the existing iteration. O shows the number of individuals:

$$H_j^u = \frac{\sum_{k=1}^{O} Y_k^u}{O} \tag{25}$$

In Eq. (25), Y_k^u refers to the velocity. The cohesion can be examined by the subsequent expression:

$$I_j^u = \frac{\sum_{k=1}^{O} Y_k^u}{O} - Y_j^u \tag{26}$$

In Eq. (26), Y_j is the existing location. k is the index. u is the existing iteration. Y_j is the individual location. Using Eq. (27), the food-searching activities are measured:

$$G_j^u = Y_+^u - Y_j^u \tag{27}$$

Where Y_+^u represents the food location, which defines the better fitness solution. Using Eq. (28), the escaping strategy can be measured:

$$Q_j^u = Y_-^u - Y_j^u \tag{28}$$

Where Y_-^u is the enemy location, which defines the worst fitness solution. Using Eq. (29), the dragonfly movement can be calculated:

$$\triangle Y_j^{u+1} = \left(tT_j^u + hH_j^u + iI_j^u + gG_j^u + qQ_j^u\right) + x \triangle Y_j^u \tag{29}$$

Where t refers to the coefficient value. T_j^u denotes the separation degree. b specifies the arrangement coefficient. H_j^u shows the individual's placement. i is the cohesion coefficient. G_j^u is the individual's cohesion. g is the food source, and the enemy is noted by q. The individual's enemy is noted by Q_j^u. x is the weight, and u is the iteration:

$$Y_j^{u+1} = Y_j^u + x \triangle Y_j^{u+1} \tag{30}$$

Where Y_j^{u+1} refers to the location vector. Using Eq. 29, the location can be updated:

$$Y_j^{(u+1)} = Y_j^u + LEVY(z) \times Y_j^u \tag{31}$$

Where u denotes the existing iteration. z is the dimension. The term $LEVY$ (y) can be evaluated as follows:

$$LEVY\ (y) = 0.01 \times \left(\frac{S_1 \times \vartheta}{|S_2|^{\frac{1}{\theta}}}\right) \tag{32}$$

Where $s1$ and $s2$ are the random values, respectively. θ is the constant value:

$$\theta = \left(\frac{\zeta(1+\theta) \times s\dot{m}\left(\frac{\pi\theta}{2}\right)}{\zeta\left(\frac{1+\theta}{2}\right) \times \theta \times 2 \times \left(\frac{\theta-1}{2}\right)}\right)^{\frac{1}{\theta}} \tag{33}$$

$$\zeta(y) = (y-1)! \tag{34}$$

In the exploration phase, the pollination activity is used. Also, it is known as the removal stage. The coefficient shows the amount of each flower's planting space near the ideal flower in this pollination type. Using Eq. (35), these behaviors are measured:

$$Y_j^{(u+1)} = Y_j^u + S\left(Y_j^u - h^*\right) \tag{35}$$

Where $Y_j^{(u+1)}$ refers to the pollen place. h^* is the fittest location. S is the area growth:

$$S = 2q^{-\left(\frac{4u}{M}\right)^2} \tag{36}$$

Where M denotes the iteration number. S is a balance between the exploration and exploitation stages:

$$i_j^u = \frac{(|g_j^u - g_{MAX}|) \times Cns}{(|g_{MIN} - g_{MAX}|)} \tag{37}$$

Where i_j^u is the capacity. g_j^u is the size, and g_{MAX} shows the largest suitable size. g_{IN} specifies the least suitable size:

$$SLCT_j^u = \frac{i_j^u}{\sum_{k=0}^{i} i_k^u} \tag{38}$$

Where l shows the number of pits. i_j^u refers to the capacity. Using Eq. (39), the drop velocity is measured:

$$W_j^{u+1} = r \times W_j^u \tag{39}$$

Using Eqs. (40) & Eq. (41), the location of moving drops can be measured:

$$W_j^{u+1} = W_j^u + rnd\left(Y_{DEp}^u - Y_j^u\right) \tag{40}$$

$$Y_j^{u+1} = Y_j^u + W_j^{u+1} \tag{41}$$

Where Y_{DEp}^u and W_j^u refer to the existing location and velocity. Fig. 2 depicts the flowchart of LEA.

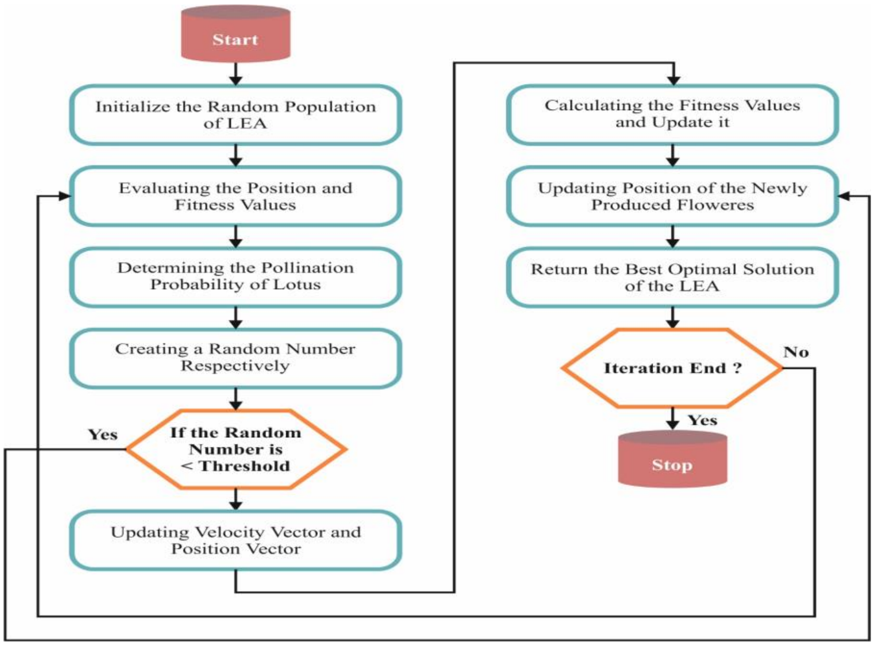

Fig. 2: Flowchart of LEA

Steps Involved in LEA-Based Routing Approach

The LEA technique selects optimal routes using a fitness function comprising link quality and power proficiency. The optimum routing tree is chosen so it reduces the cost of the objective function (Elhabyan and Yagoub, 2015). To achieve an energy-efficient routing tree, dual supporting objectives should be faced:

(1) Save Energy: Some SNs should be active at all the rounds. To accomplish that, the protocol should favor CHs and relay nodes as the best candidates to perform as a relay node:

$$EE(a)_p = \frac{R}{c} \tag{42}$$

(2) Balance energy consumption: Relay nodes with maximum energy are the fittest candidates to be included in the routing tree. Eq. (43) is used for balancing the energy usage amongst the network nodes:

$$EE(b)_p = \frac{\sum_{i=1}^{N} E(n_i)}{\sum_{r=1}^{R} E(RN_{p,r})} \tag{43}$$

To increase the PRR, the procedure should increase the connection excellence among the relay nodes. The following function reduces the worst connection quality among each branch in the routing tree as follows:

$$LQ_p = \max_{b=1,2,\ldots,R} \sum_{\forall rn_i \in r} \frac{RSSI(rn_i, rn_{i+1})}{\min RSSI} \tag{44}$$

After evaluating the prior secondary objectives, the last objective function that should be reduced:

$$R_p = wr_1 \times EE(a)_p + wr_2 \times EE(b)_p + wr_3 \times LQ_p \tag{45}$$

Computational Complexity Analysis

The weighting parameters p, q, and r were used to balance the effects of various clustering objectives (preserving residual energy, minimizing communication distance, and balancing efficiency of the clusters). These weighting coefficients are carefully selected to avoid premature exhaustion of the energy of cluster heads and to distribute the energy evenly among cluster heads. The proposed weighting method ensures the stability of the cluster and maximizes the network lifetime by taking into account both the communication efficiency and the energy condition of nodes simultaneously. The proposed MBCRP-LFTM framework primarily relies on two optimization techniques: IEMOA (clustering optimization) and LEA (routing optimization), whose computational complexities are the main concerns.

The complexity of the IEMOA-based clustering phase is related to position initialization, complexity of fitness evaluation, and iterative position updating. Let the number of sensor nodes be denoted as N, the population size as P, and the maximum number of iterations as I. The complexity of IEMOA can be approximated to:

$$O(P \times N \times I)$$

In the same manner, for the routing stage based on LEA, the optimization of the routes is repeated, evaluating the routing candidates and modifying the optimal selection of relays. If there are n routing candidates (denoted 'ras' and t as the number of iterations, then the complexity of LEA can be written as:

$$O(R \times N \times T)$$

The computational complexity of the MBCRP-LFTM framework is thus dependent on both clustering and routing optimization stages. However, the approach proposed is executed sequentially, which minimizes the total computation overhead and makes it suitable for a resource-constrained WSN environment for the clustering and routing operations.

Performance Validation

This template, created in MS Word 2003 and saved as "Word 97-2003 & 6.0/95-RTF" for the PC, provides authors with most of the formatting specifications given in the instructions to authors and needed for preparing electronic versions of their papers. All standard paper components have been specified for three reasons:

(a) Ease of use when formatting individual papers
(b) Automatic compliance with electronic requirements that facilitate the production of electronic products
(c) Conformity of style throughout a journal paper. Margins, line spacing, and type styles are built-in. Examples of the type styles are provided throughout this document and are identified in type, within parentheses

This section analyzes the performance validation of the MBCRP-LFTM method in terms of dissimilar measures. The outcomes are inspected under four distinct scenarios defined in Table 1.

Different WSN deployment conditions (small-scale and large-scale sensor environments) are represented by choosing the simulation parameters and network configurations. Various network sizes, sensor node densities, and initial battery energy levels are taken into consideration to assess the scalability, robustness, and energy efficiency properties of the proposed MBCRP-LFTM framework in different communication scenarios.

In Table 2, the comparative number of alive nodes (NOAN) study of the MBCRP-LFTM method under S-1 is established (Soundararajan et al., 2024). The results indicate the superior energy efficiency of the MBCRP-LFTM system. With 600 rounds, the MBCRP-LFTM method provides a higher NOAN of 99, while the LEACH, URBD, DEFL, E-FUCA, and FLHBA approaches get lower NOAN of 69, 87, 96, 97, and 98, respectively. Likewise, with 1000 rounds, the MBCRP-LFTM model offers a higher NOAN of 98, whereas the LEACH, URBD, DEFL, E-FUCA, and FLHBA techniques get lower NOAN of 34, 57, 66, 85, and 97, respectively. Meanwhile, with 1500 rounds, the MBCRP-LFTM model offers a better NOAN of 73, whereas the LEACH, URBD, DEFL, E-FUCA, and FLHBA approaches attain lower NOAN of 5, 11, 24, 41, and 67, respectively.

In Table 3, the comparative NOAN analysis of the MBCRP-LFTM system under S-2 is demonstrated. The outcomes specify the higher energy efficiency results of the MBCRP-LFTM system. With 600 rounds, the MBCRP-LFTM approach provides a higher NOAN of 198, while the LEACH, URBD, DEFL, E-FUCA, and FLHBA approaches attain lower NOAN of 135, 161, 191, 194, and 197, respectively. Similarly, with 1000 rounds, the MBCRP-LFTM technique delivers a higher NOAN of 188, while the LEACH, URBD, DEFL, E-FUCA, and FLHBA approaches get lower NOAN of 68, 99, 123, 123, and 186, respectively. In the meantime, with 1500 rounds, the MBCRP-LFTM method offers a higher NOAN of 127, whereas the LEACH, URBD, DEFL, E-FUCA, and FLHBA techniques achieve lower NOAN of 12, 15, 44, 45, and 124, respectively.

In Table 4, the comparative NOAN analysis of the MBCRP-LFTM system under S-3 is revealed. The outcomes specify the higher energy efficiency results of the MBCRP-LFTM approach. With 600 rounds, the MBCRP-LFTM system provides a higher NOAN of 299, whereas the LEACH, URBD, DEFL, E-FUCA, and FLHBA approaches get lower NOAN of 194, 247, 271, 276, and 298, respectively. Likewise, with 1000 rounds, the MBCRP-LFTM system provides a higher NOAN of 284, whereas the LEACH, URBD, DEFL, E-FUCA, and FLHBA approaches get lower NOAN of 90, 159, 198, 262, and 277, correspondingly.

Table 1: Simulation setup

Parameters	Symbol	Scenario-1	Scenario-2	Scenario-3	Scenario-4
Total SN	N	100	200	300	500
Area	A	(200, 200)	(200, 200)	(300, 300)	(500, 500)
BS location	BS	(300, 100)	(100, 100)	(150, 0)	(500, 0)
Free-space model	ϵ_{fs}	10 pJ/bit/m^2	10 pJ/bit/m^2	10 pJ/bit/m^2	10 pJ/bit/m^2
Multipath model	ϵ_{mp}	0.0013 pJ/bit/m^4	0.0013 pJ/bit/m^4	0.0013 pJ/bit/m^4	0.0013 pJ/bit/m^4
Initial battery level	E_o	1 J	0.5 J	0.5 J	0.5 J
Size of packet	M	4000 bits	4000 bits	4000 bits	4000 bits
Data aggregation	E_{DA}	5 nJ/bit/report	5 nJ/bit/report	5 nJ/bit/report	5 nJ/bit/report
Electronic circuitry	E_{elec}	50 nJ/bit	50 nJ/bit	50 nJ/bit	50 nJ/bit

Table 2: NOAN result of MBCRP-LFTM model along with existing models from S-1

Number of Alive Nodes: Scenario-1						
No. of Rounds	LEACH Protocol	URBD Protocol	DEFL Protocol	E-FUCA Protocol	FLHBA-CMHR	MBCRP-LFTM
0	100	100	100	100	100	100
100	99	98	98	99	99	99
200	98	98	98	99	99	99
300	93	97	98	99	99	99
400	90	97	98	98	99	99
500	76	95	97	98	99	99
600	69	87	96	97	98	99
700	60	83	92	98	98	99
800	53	77	83	96	98	99
900	37	68	76	92	98	98
1000	34	57	66	85	97	98
1100	27	51	57	73	91	98
1200	25	37	48	65	83	98
1300	19	24	40	58	77	84
1400	9	18	36	49	73	79
1500	5	11	24	41	67	73
1600	7	8	18	31	56	62
1700	5	8	13	26	50	57
1800	5	6	8	19	49	56
1900	0	0	6	12	42	48
2000	0	0	6	9	36	43
2100	0	0	0	5	27	33
2200	0	0	0	0	15	22
2300	0	0	0	0	0	6
2400	0	0	0	0	0	0
2500	0	0	0	0	0	0

Table 3: NOAN result of MBCRP-LFTM method with existing models from S-2

Number of Alive Nodes: Scenario-2						
No. of Rounds	LEACH Protocol	URBD Protocol	DEFL Protocol	E-FUCA Protocol	FLHBA-CMHR	MBCRP-LFTM
0	200	200	200	200	200	200
100	198	198	197	199	199	199
200	197	197	198	199	198	199
300	185	193	196	198	198	199
400	173	187	199	199	196	198
500	150	168	194	197	196	198
600	135	161	191	194	197	198
700	117	147	178	183	196	197
800	102	131	160	169	197	198
900	72	112	146	139	192	194
1000	68	99	123	123	186	188
1100	52	70	108	112	178	181
1200	40	46	94	94	156	158
1300	35	32	77	76	148	150
1400	18	23	64	62	139	141
1500	12	15	44	45	124	127
1600	9	9	29	32	109	111
1700	6	10	24	26	95	97
1800	4	7	13	12	95	98
1900	0	9	10	7	82	84
2000	0	7	4	8	68	71
2100	0	7	5	7	51	54
2200	0	4	3	3	25	27
2300	0	3	4	2	25	27
2400	0	0	0	0	23	26
2500	0	0	0	0	0	0

Table 4: NOAN outcome of MBCRP-LFTM technique with existing models under S-3

Number of Alive Nodes: Scenario-3						
No. of Rounds	LEACH Protocol	URBD Protocol	DEFL Protocol	E-FUCA Protocol	FLHBA-CMHR	MBCRP-LFTM
0	300	300	300	300	300	300
100	300	300	300	300	300	300
200	284	294	297	297	300	300
300	280	301	296	296	300	300
400	253	292	285	290	297	300
500	226	285	281	288	297	300
600	194	247	271	276	298	299
700	187	207	254	282	295	299
800	159	208	228	274	291	298
900	96	167	204	264	284	292
1000	90	159	198	262	277	284
1100	73	145	152	205	254	260
1200	66	114	125	177	240	248
1300	53	106	123	168	209	216
1400	27	92	94	144	200	208
1500	18	84	68	98	179	185
1600	15	52	51	96	172	180
1700	13	33	42	66	138	145
1800	13	32	38	54	137	142
1900	9	28	33	49	126	131
2000	8	29	29	41	114	121
2100	6	17	31	33	83	91
2200	0	7	27	33	36	41
2300	0	5	24	27	28	33
2400	0	0	11	24	28	35
2500	0	0	0	0	0	0

Meanwhile, with 1500 rounds, the MBCRP-LFTM method provides a higher NOAN of 185, whereas the LEACH, URBD, DEFL, E-FUCA, and FLHBA systems get lower NOAN of 18, 84, 68, 98, and 179, correspondingly.

In Table 5, the comparative NOAN study of the MBCRP-LFTM method under S-4 is established. The outcome designates the greater energy efficiency results of the MBCRP-LFTM system. With 600 rounds, the MBCRP-LFTM approach achieves a higher NOAN of 500, whereas the LEACH, URBD, DEFL, E-FUCA, and FLHBA methods accomplish lower NOAN of 343, 418, 476, 474, and 493, respectively. Additionally, with 1000 rounds, the MBCRP-LFTM approach delivers a high NOAN of 458, whereas the LEACH, URBD, DEFL, E-FUCA, and FLHBA systems get lower NOAN of 153, 289, 285, 435, and 449, respectively. Meanwhile, with 1500 rounds, the MBCRP-LFTM technique offers a better NOAN of 308, whereas the LEACH, URBD, DEFL, E-FUCA, and FLHBA models get lower NOAN of 24, 130, 79, 177, and 298, respectively.

In Fig. 3, the overall NOAN outcomes of the MBCRP-LFTM system with current methods are demonstrated. The results establish that the MBCRP-LFTM method achieves better performance under all scenarios.

In Table 6, the comparative Residual Energy (RE) analysis of the MBCRP-LFTM technique under S-1 is demonstrated. The results indicate the superior energy efficiency outcomes of the MBCRP-LFTM technique. With 100 rounds, the MBCRP-LFTM technique offers higher RE of 99J, whereas the LEACH, URBD, DEFL, E-FUCA, and FLHBA systems get lower RE of 97J, 96J, 96J, 97J, and 97J, correspondingly. Also, with 500 rounds, the MBCRP-LFTM system provides a greater RE of 99J, whereas the LEACH, URBD, DEFL, E-FUCA, and FLHBA systems attain lower RE of 73J, 90J, 95J, 96J, and 98J, respectively. Meanwhile, with 1000 rounds, the MBCRP-LFTM method achieves a higher RE of 95J, while the LEACH, URBD, DEFL, E-FUCA, and FLHBA approaches get lower RE of 32J, 54J, 61J, 81J, and 91J, respectively.

In Table 7, the comparative RE analysis of the MBCRP-LFTM method under S-2 is demonstrated. The outcomes specify the superior energy efficiency results of the MBCRP-LFTM approach. With 100 rounds, the MBCRP-LFTM model provides offers a higher RE of 149J, whereas the LEACH, URBD, DEFL, E-FUCA, and FLHBA techniques attain lower REs of 149J, 149J, 148J, 149J, and 149J, respectively. Besides, with 500 rounds, the MBCRP-LFTM models provides a better RE of 149J while the LEACH, URBD, DEFL, E-FUCA, and FLHBA models get lower RE of 110J, 140J, 144J, 148J, and 148J, respectively. Meanwhile, with 1000 rounds, the MBCRP-LFTM system gets a greater RE of 148J whereas the LEACH, URBD, DEFL, E-FUCA, and FLHBA systems get lesser RE of 48J, 83J, 92J, 124J, and 139J, correspondingly.

Table 5: NOAN result of MBCRP-LFTM technique along with existing technique from S-4

Number of Alive Nodes: Scenario-4						
No. of Rounds	LEACH Protocol	URBD Protocol	DEFL Protocol	E-FUCA Protocol	FLHBA-CMHR	MBCRP-LFTM
0	500	500	500	500	500	500
100	497	495	495	498	500	500
200	474	488	495	498	500	500
300	447	480	496	498	500	500
400	427	475	497	498	500	500
500	373	454	484	488	497	500
600	343	418	476	474	493	500
700	285	386	432	474	482	499
800	224	343	411	463	473	498
900	167	340	384	448	469	498
1000	153	289	285	434	449	458
1100	142	220	285	349	423	432
1200	102	200	222	324	414	422
1300	98	175	180	255	363	372
1400	35	142	146	242	332	340
1500	24	130	79	177	298	308
1600	24	50	69	172	295	305
1700	23	44	55	91	212	220
1800	18	19	45	86	210	220
1900	20	19	44	47	207	215
2000	15	12	39	37	142	150
2100	0	8	24	34	115	124
2200	0	0	9	28	57	65
2300	0	0	7	9	44	53
2400	0	0	0	7	27	35
2500	0	0	0	0	0	0

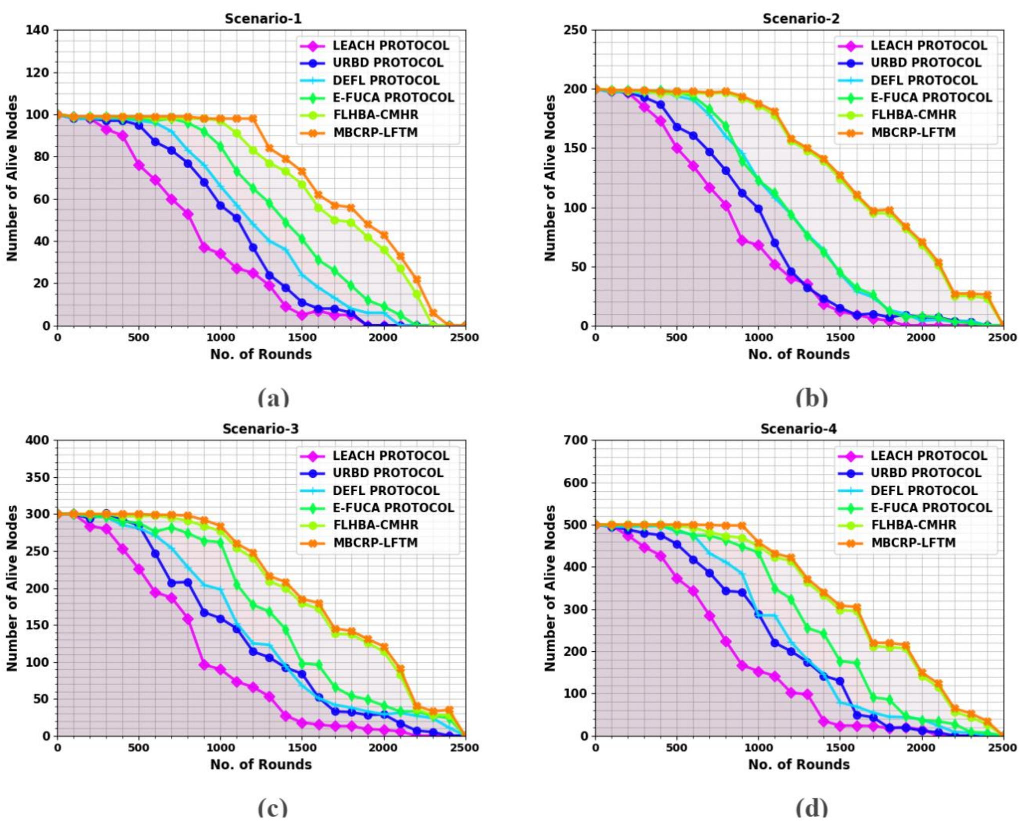

Fig. 3: NOAN outcome of MBCRP-LFTM technique (a-d) Scenario 1-4

DOI: 10.3844/jcssp.2026.2236.2253

Table 6: RE result of MBCRP-LFTM technique with existing models from S-1

Energy of Network (Joules): Scenario-1						
No. of Rounds	LEACH Protocol	URBD Protocol	DEFL Protocol	E-FUCA Protocol	FLHBA-CMHR	MBCRP-LFTM
0	100	100	100	100	100	100
100	97	96	96	97	97	99
200	97	97	97	97	97	98
300	90	96	97	97	97	98
400	84	95	97	97	97	98
500	73	90	95	96	98	99
600	66	84	92	95	97	98
700	56	78	88	97	97	98
800	48	73	79	95	96	97
900	34	63	73	89	93	96
1000	32	54	61	81	91	95
1100	25	49	54	69	87	92
1200	21	34	45	60	78	89
1300	16	21	39	53	74	85
1400	9	15	32	47	68	78
1500	5	10	21	37	61	71
1600	5	7	16	30	53	64
1700	4	4	10	22	48	58
1800	3	4	8	17	46	56
1900	2	0	5	11	40	50
2000	0	0	4	6	34	44
2100	0	0	0	4	24	35
2200	0	0	0	0	13	25
2300	0	0	0	0	0	10
2400	0	0	0	0	0	0
2500	0	0	0	0	0	0

Table 7: RE outcome of MBCRP-LFTM technique with existing methods under S-2

Energy of Network (Joules): Scenario-2						
No. of Rounds	LEACH Protocol	URBD Protocol	DEFL Protocol	E-FUCA Protocol	FLHBA-CMHR	MBCRP-LFTM
0	150	150	150	150	150	150
100	149	149	148	149	149	149
200	147	148	148	149	149	149
300	139	146	148	149	149	149
400	127	145	147	148	149	149
500	110	140	144	148	148	149
600	100	126	142	148	149	149
700	88	121	133	148	148	148
800	75	110	121	144	148	148
900	52	98	108	135	144	148
1000	48	83	92	124	139	148
1100	38	73	81	103	134	155
1200	30	50	69	92	117	137
1300	26	33	58	83	111	151
1400	12	24	48	70	102	133
1500	7	16	31	55	93	120
1600	6	10	21	46	81	103
1700	5	6	16	33	70	105
1800	3	7	10	24	70	95
1900	0	5	6	19	60	95
2000	0	5	4	6	51	75
2100	0	4	3	6	36	72
2200	0	3	2	6	16	48
2300	0	2	2	2	16	42
2400	0	0	0	0	16	46
2500	0	0	0	0	0	0

In Table 8, the comparative RE analysis of the MBCRP-LFTM technique under S-3 is demonstrated. The results indicate the superior energy efficacy outcomes of the MBCRP-LFTM technique. With 100 rounds, the MBCRP-LFTM technique offers a higher RE of 145J during the LEACH, URBD, DEFL, E-FUCA, and FLHBA models achieve lower RE of 137J, 137J, 136J, 136J, and 136J, correspondingly. Also, with 500 rounds, the MBCRP-LFTM approach delivers a higher RE of 144J where the LEACH, URBD, DEFL, E-FUCA, and FLHBA approaches get lower RE of 102J, 129J, 126J, 129J, and 135J, correspondingly. Meanwhile, with 1000 rounds, MBCRP-LFTM methods offers a higher RE of 133J whereas the LEACH, URBD, DEFL, E-FUCA, and FLHBA methodologies achieve lower RE of 40J, 73J, 90J, 119J, and 128J, correspondingly.

In Table 9, the comparative RE analysis of the MBCRP-LFTM technique under S-4 is demonstrated. The results indicate the superior energy efficacy outcomes of the MBCRP-LFTM technique. With 100 rounds, the MBCRP-LFTM method offers a higher RE of 99J whereas the LEACH, URBD, DEFL, E-FUCA, and FLHBA approaches gy lower RE of 97J, 96J, 96J, 97J, and 97J, correspondingly. Also, with 500 rounds, the MBCRP-LFTM systems reaches a higher RE of 99J whereas the LEACH, URBD, DEFL, E-FUCA, and FLHBA systems reach lower RE of 73J, 90J, 95J, 96J, and 98J, correspondingly. Meanwhile, with 1000 rounds, the MBCRP-LFTM model offers a higher RE of 95J where the LEACH, URBD, DEFL, E-FUCA, and FLHBA approaches achieve lower RE of 32J, 54J, 61J, 81J, and 91J, correspondingly.

In Fig. 4, the whole energy efficiency results of the MBCRP-LFTM method with recent models are demonstrated. The outcomes establish that the MBCRP-LFTM system reaches superior performance under all scenarios.

In Table 10, the FND results of the MBCRP-LFTM system with existing methodologies are portrayed. The results designate that the MBCRP-LFTM technique has exhibited higher FND values. For instance, on S1, the MBCRP-LFTM approach gives a better FND of 421 rounds during the LEACH, URBD, DEFL, E-FUCA, and FLHBA models obtain lower FND of 165, 182, 185, 196, and 395, correspondingly. Besides, on S4, the MBCRP-LFTM system gets a maximum FND of 499 rounds while the LEACH, URBD, DEFL, E-FUCA, and FLHBA models obtain lower FND of 98, 99, 99, 99, and 498, correspondingly.

Table 8: RE outcome of MBCRP-LFTM technique with existing methods from S-3

Energy of Network (Joules): Scenario-3						
No. of Rounds	LEACH Protocol	URBD Protocol	DEFL Protocol	E-FUCA Protocol	FLHBA-CMHR	MBCRP-LFTM
0	150	150	150	150	150	150
100	137	137	136	136	136	145
200	128	133	133	136	137	144
300	127	136	134	134	137	143
400	114	131	127	131	136	145
500	102	129	126	129	135	144
600	87	111	123	124	133	142
700	85	93	115	128	133	140
800	72	94	102	123	130	138
900	44	75	91	119	128	135
1000	40	73	90	119	124	133
1100	33	65	69	92	115	123
1200	29	52	56	81	109	117
1300	25	48	55	76	95	103
1400	13	42	42	64	90	97
1500	8	37	31	43	81	87
1600	6	23	23	44	78	85
1700	6	16	19	31	63	72
1800	6	14	18	24	63	70
1900	5	14	16	22	57	62
2000	3	13	13	19	52	60
2100	2	9	13	15	38	47
2200	0	4	13	15	15	20
2300	0	3	11	13	13	19
2400	0	0	5	10	14	21
2500	0	0	0	0	0	0

DOI: 10.3844/jcssp.2026.2236.2253

Table 9: RE outcome of MBCRP-LFTM technique with existing methods under S-4

Energy of Network (Joules): Scenario-4						
No. of Rounds	LEACH Protocol	URBD Protocol	DEFL Protocol	E-FUCA Protocol	FLHBA-CMHR	MBCRP-LFTM
0	250	250	250	250	250	250
100	222	224	226	228	226	238
200	214	220	221	222	226	237
300	201	217	219	220	226	237
400	193	214	215	217	226	239
500	168	205	206	208	225	239
600	154	188	189	191	221	233
700	127	172	174	175	217	231
800	101	153	154	156	212	226
900	74	152	153	154	210	224
1000	70	129	131	133	201	213
1100	64	99	101	103	191	204
1200	47	90	91	93	187	197
1300	44	79	80	82	162	174
1400	15	65	66	68	149	160
1500	10	59	60	61	134	144
1600	11	23	24	26	132	146
1700	11	20	21	22	95	110
1800	8	9	10	11	93	104
1900	8	8	9	11	93	108
2000	7	5	7	8	64	77
2100	0	3	4	5	52	66
2200	0	0	1	3	26	38
2300	0	0	1	2	20	34
2400	0	0	0	1	12	27
2500	0	0	0	0	0	0

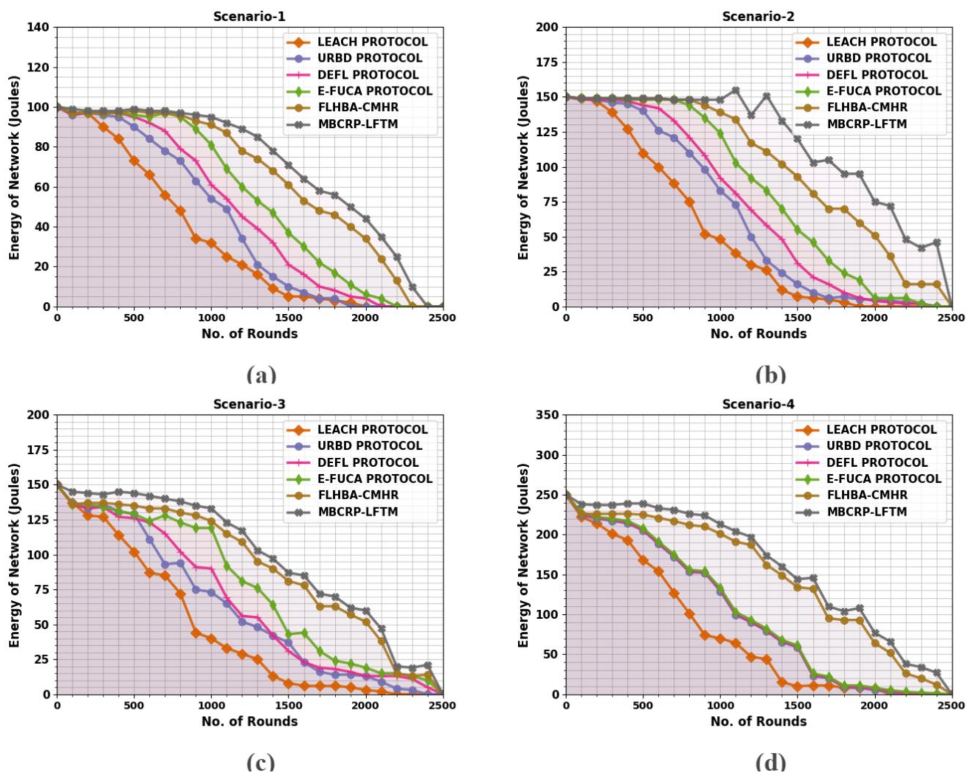

Fig. 4: Energy efficiency outcome of MBCRP-LFTM technique (a-d) Scenario 1-4

Table 10: FND outcome of MBCRP-LFTM technique with existing methods under various scenario

FND						
Scenario	LEACH Protocol	URBD Protocol	DEFL Protocol	E-FUCA Protocol	FLHBA-CMHR	MBCRP-LFTM
Scenario-1	98	98	98	99	99	99
Scenario-2	97	97	98	99	100	100
Scenario-3	165	182	185	196	395	421
Scenario-4	98	99	99	99	498	499

In Table 11, the QND results of the MBCRP-LFTM technique with existing methods are portrayed. The outcomes specify that the MBCRP-LFTM system has exhibited higher QND values. For example, on S1, the MBCRP-LFTM model offers higher QND of 1561 rounds whereas the LEACH, URBD, DEFL, E-FUCA, and FLHBA tehui get lower QND of 509, 806, 902, 1050, and 1312, correspondingly. Besides, on S4, the MBCRP-LFTM models gives a higher QND of 1518 rounds where the LEACH, URBD, DEFL, E-FUCA, and FLHBA models obtain lower QND of 510, 724, 922, 1086, and 1307, correspondingly.

In Table 12, the HND outcomes of the MBCRP-LFTM model with present systems are portrayed. The results indicate that the MBCRP-LFTM techniques has display greater HND values. For example, on S1, the MBCRP-LFTM systems gives a greater HND of 1945 rounds where the LEACH, URBD, DEFL, E-FUCA, and FLHBA models obtain lower HND of 805, 1110, 1167, 1364, and 1691, correspondingly. Besides, on S4, the MBCRP-LFTM algorithm delivers a higher HND of 1927 rounds during the LEACH, URBD, DEFL, E-FUCA, and FLHBA models obtain lower HND of 760, 1063, 1174, 1310, and 1680, correspondingly. Therefore, the MBCRP-LFTM technique can be applied for improved network lifetime in WSN. The balanced unequal clustering strategy and adaptive energy-aware routing optimization are mainly responsible for the superior performance of the MBCRP-LFTM framework. The clustering mechanism based on IEMOA is effective to distribute communication load among cluster heads, to reduce premature node fails. At the same time, the LEA-based routing model chooses the optimal communication paths with better link quality and life time awareness property. The proposed framework, therefore, results in more alive nodes, better residual energy preservation, and longer network lifetime in all of the simulation scenarios than current solutions.

Table 11: QND outcome of MBCRP-LFTM technique with existing methods under various scenarios

QND						
Scenario	LEACH Protocol	URBD Protocol	DEFL Protocol	E-FUCA Protocol	FLHBA-CMHR	MBCRP-LFTM
Scenario-1	509	806	902	1050	1312	1561
Scenario-2	513	802	893	1041	1291	1613
Scenario-3	514	676	814	1099	1261	1582
Scenario-4	510	724	922	1086	1307	1518

Table 12: HND outcome of MBCRP-LFTM technique with existing methods under various scenarios

HND						
Scenario	LEACH Protocol	URBD Protocol	DEFL Protocol	E-FUCA Protocol	FLHBA-CMHR	MBCRP-LFTM
Scenario-1	805	1110	1167	1364	1691	1945
Scenario-2	803	1107	1153	1354	1644	1879
Scenario-3	836	1140	1114	1403	1682	1989
Scenario-4	760	1063	1174	1310	1680	1927

Conclusion

In the study, we have proposed a novel MBCRP-LFTM technique in WSN. The presented MBCRP-LFTM technique enhances energy proficiency and lifespan of WSN employing cluster-driven routing approaches. In the MBCRP-LFTM technique, the IEMOA-based clustering technique is presented for effective CH collection and unequal cluster creation. Also, the IEMOA-based clustering method designs an objective function comprising multiple input metrics such as residual power level, CH balancing factor, inter and intra-cluster distance. Meanwhile, the MBCRP-LFTM technique designs LEA-based routing methods to pick optimum routes to sink. The LEA technique selects optimal routes using a fitness function comprising energy efficiency and link quality. An extensive series of simulations was led to demonstrate the presentation of MBCRP-LFTM technique. The experimental outcomes reported, which MBCRP-LFTM system accomplishes improved performance than other recent approaches. The proposed model—MBCRP-LFTM framework can provide better performance for WSNs in static environments; for future work, the proposed model can be extended to dynamic network situations where the sensor nodes can be mobile, the energy of sensor nodes can be heterogeneous, and the topology can be changed adaptively. Moreover, future improvement can be achieved by introducing fault-tolerant routing techniques, security-based communication protocols, and adaptive optimization for real-time applications with IoT integration in a WSN. Further study could also involve real-time implementation with hardware and deployment in a real application scenario with embedded WSN platforms of the proposed MBCRP-LFTM framework. The proposed protocol can be further validated under experimental conditions in real communication environments for application in industrial monitoring, healthcare systems, smart agriculture, and IoT based on sensing applications.

Data Availability Statement

The authors confirm that the data supporting the findings of this study are available within the article (Soundararajan et al., 2024).

Acknowledgment

The authors would like to express their sincere gratitude to the Department of Information Technology, FEAT, Annamalai University, for providing the necessary research facilities and support to carry out this work.

Funding Information

The authors declare that no specific funding was received from any government agency, commercial organization, or non-profit funding body for conducting this research work.

Author's Contributions

N. E. Kanaghadhara: Contributed to the conceptualization, methodology development, simulation, analysis, implementation, and manuscript preparation.

R. Suban: Contributed to supervision, validation, review, editing, and overall guidance of the research work.

Ethic

This article does not contain any studies involving human participants or animals performed by any of the authors.

References

Abidi, M. H., Chintakindi, S., Rehman, A. U., & Mohammed, M. K. (2024). Performance enhancement in hydroponic and soil compound prediction by deep learning techniques. *PeerJ Computer Science*, *10*, e2101. https://doi.org/10.7717/peerj-cs.2101

Arjunan, S., & Pothula, S. (2019). A survey on unequal clustering protocols in Wireless Sensor Networks. *Journal of King Saud University - Computer and Information Sciences*, *31*(3), 304–317. https://doi.org/10.1016/j.jksuci.2017.03.006

Arjunan, S., & Sujatha, P. (2018). Lifetime maximization of wireless sensor network using fuzzy based unequal clustering and ACO based routing hybrid protocol. *Applied Intelligence 48*(8), 2229–2246. https://doi.org/10.1007/s10489-017-1077-y

Barnwal, S. K., Prakash, A., & Yadav, D. K. (2023). Improved African Buffalo Optimization-Based Energy Efficient Clustering Wireless Sensor Networks using Metaheuristic Routing Technique. *Wireless Personal Communications*, *130*(3), 1575–1596. https://doi.org/10.1007/s11277-023-10345-z

Chaurasia, S., & Kumar, K. (2023). MOORP: Metaheuristic Based Optimized Opportunistic Routing Protocol for Wireless Sensor Network. *Wireless Personal Communications 132*(2), 1241–1272. https://doi.org/10.1007/s11277-023-10659-y

Cherappa, V., Thangarajan, T., Meenakshi Sundaram, S. S., Hajjej, F., Munusamy, A. K., & Shanmugam, R. (2023). Energy-Efficient Clustering and Routing Using ASFO and a Cross-Layer-Based Expedient Routing Protocol for Wireless Sensor Networks. *Sensors*, *23*(5), 2788. https://doi.org/10.3390/s23052788

Daniel, A., Balamurugan, K. M., Vijay, R., & Arjun, K. P. (2021). Energy Aware Clustering with Multihop Routing Algorithm for Wireless Sensor Networks. *Intelligent Automation & Soft Computing*, *29*(1), 233–246. https://doi.org/10.32604/iasc.2021.016405

Darabkh, K. A., El-Yabroudi, M. Z., & El-Mousa, A. H. (2019). BPA-CRP: A balanced power-aware clustering and routing protocol for wireless sensor networks. *Ad Hoc Networks*, *82*, 155–171. https://doi.org/10.1016/j.adhoc.2018.08.012

Elhabyan, R. S. Y., & Yagoub, M. C. E. (2015). Two-tier particle swarm optimization protocol for clustering and routing in wireless sensor network. *Journal of Network and Computer Applications*, *52*, 116–128. https://doi.org/10.1016/j.jnca.2015.02.004

Fang, W., Zhang, W., Yang, W., Li, Z., Gao, W., & Yang, Y. (2021). Trust management-based and energy efficient hierarchical routing protocol in wireless sensor networks. *Digital Communications and Networks*, *7*(4), 470–478. https://doi.org/10.1016/j.dcan.2021.03.005

He, S., Li, Q., Khishe, M., Salih Mohammed, A., Mohammadi, H., & Mohammadi, M. (2024). The Optimization of Nodes Clustering and Multi-Hop Routing Protocol Using Hierarchical Chimp Optimization for Sustainable Energy Efficient Underwater Wireless Sensor Networks. *Wireless Networks*, *30*(1), 233–252. https://doi.org/10.1007/s11276-023-03464-9

Kumar Dutta, A., Albagory, Y., Alsanea, M., Sait, A. R. W., & AlRawashdeh, H. S. (2023). Fuzzy with Metaheuristics Based Routing for Clustered Wireless Sensor Networks. *Intelligent Automation & Soft Computing*, *35*(1), 367–380. https://doi.org/10.32604/iasc.2023.027076

Mohan, P., Subramani, N., Alotaibi, Y., Alghamdi, S., Khalaf, O. I., & Ulaganathan, S. (2022). Improved Metaheuristics-Based Clustering with Multihop Routing Protocol for Underwater Wireless Sensor Networks. *Sensors*, *22*(4), 1618. https://doi.org/10.3390/s22041618

Ramachandran, N., & Perumal, V. (2018). Delay-aware heterogeneous cluster-based data acquisition in Internet of Things. *Computers & Electrical Engineering*, *65*, 44–58. https://doi.org/10.1016/j.compeleceng.2017.03.018

Rao, M. R., & Sundar, S. (2024). Enhancement in Optimal Resource-Based Data Transmission Over LPWAN Using a Deep Adaptive Reinforcement Learning Model Aided by Novel Remora With Lotus Effect Optimization Algorithm. *IEEE Access*, *12*, 76515–76531. https://doi.org/10.1109/access.2024.3406749

Roberts, M. K., Thangavel, J., & Aldawsari, H. (2024). An improved dual-phased meta-heuristic optimization-based framework for energy efficient cluster-based routing in wireless sensor networks. *Alexandria Engineering Journal*, *101*, 306–317. https://doi.org/10.1016/j.aej.2024.05.078

Sahoo, B. M., & Sabyasachi, A. S. (2024). A Metaheuristic Algorithm Based Clustering Protocol for Energy Harvesting in IoT-Enabled WSN. *Wireless Personal Communications*, *136*(1), 385–410. https://doi.org/10.1007/s11277-024-11270-5

Sharma, S., Puthal, D., Jena, S. K., Zomaya, A. Y., & Ranjan, R. (2017). Rendezvous based routing protocol for wireless sensor networks with mobile sink. *Journal of Supercomputing*, *73*, 1168–1188. https://doi.org/10.1007/s11227-016-1801-0

Soundararajan, S., Kurangi, C., Basha, A., & Ahamed, S. banu. (2024). Fuzzy logic with honey badger algorithm for cluster-based multi-hop routing protocol for wireless sensor networks. *International Journal of Communication Systems*, *37*(12), e5810. https://doi.org/10.1002/dac.5810

Subramani, N., Mohan, P., Alotaibi, Y., Alghamdi, S., & Khalaf, O. I. (2022). An Efficient Metaheuristic-Based Clustering with Routing Protocol for Underwater Wireless Sensor Networks. *Sensors*, *22*(2), 415. https://doi.org/10.3390/s22020415

Tam, N. T., Hai, D. T., Son, L. H., & Vinh, L. T. (2018). Improving lifetime and network connections of 3D wireless sensor networks based on fuzzy clustering and particle swarm optimization. *Wireless Networks*, *24*, 1477–1490. https://doi.org/10.1007/s11276-016-1412-y

Tandon, A., Kumar, P., Rishiwal, V., Yadav, M., & Yadav , P. (2021). A Bio-inspired Hybrid Cross-Layer Routing Protocol for Energy Preservation in WSN-Assisted IoT. *KSII Transactions on Internet and Information Systems*, *15*(4), 1317–1341. https://doi.org/10.3837/tiis.2021.04.008

Vaiyapuri, T., Parvathy, V. S., Manikandan, V., Krishnaraj, N., Gupta, D., & Shankar, K. (2022). A Novel Hybrid Optimization for Cluster-Based Routing Protocol in Information-Centric Wireless Sensor Networks for IoT Based Mobile Edge Computing. *Wireless Personal Communications*, *127*(1), 39–62. https://doi.org/10.1007/s11277-021-08088-w

Wang, J., Wang, K., Niu, J., & Liu, W. (2018). A K-medoids based clustering algorithm for wireless sensor networks. *Proceedings of the 2018 International Workshop on Advanced Image Technology (IWAIT)*, 1–4. https://doi.org/10.1109/iwait.2018.8369769